Scientific Research Publishing

Open Journal of Microphysics, 2025, 15(3), 52-63
https://www.scirp.org/journal/ojm
ISSN Online: 2162-2469
ISSN Print: 2162-2450

Double Differential Cross Section of First Born for H (3S) by Electron Impact

Fahadul Islam*, **Sushmita Banerjee**, **Sunil Dhar**

Department of Mathematics, Chittagong University of Engineering and Technology, Chittagong, Bangladesh
Email: *fahadulislambgd@gmail.com, sushmita@cuet.ac.bd, sdhar@cuet.ac.bd

How to cite this paper: Islam, F., Banerjee, S. and Dhar, S. (2025) Double Differential Cross Section of First Born for H (3S) by Electron Impact. *Open Journal of Microphysics*, **15**, 52-63.
https://doi.org/10.4236/ojm.2025.153004

Received: June 6, 2025
Accepted: August 24, 2025
Published: August 27, 2025

Abstract

The Double Differential Cross Section (DDCS) based on the first-born approximation is computed for the ionization of metastable 3S-state hydrogenic atoms by electron impact at incident energies of 250 eV and 150 eV. A multiple scattering theory is employed in this study. The results are compared with theoretical predictions for the ionization of hydrogen atoms in the 2S and 3d states, as well as with the ground state experimental data. The findings show strong qualitative agreement with those of previously reported results. The present outcomes offer significant potential for further investigation of the ionization process.

Keywords

Ionization, Cross Sections, Electron, Scattering

1. Introduction

The ionization process is one of the most significant reactions in atomic collisions. The study of multiple ionization processes of metastable atoms by electron impact is of considerable importance across various experimental fields, including astrophysics, plasma physics, radiation physics, and applied mathematics. A central challenge in this area lies in developing a general theoretical framework that can reliably predict ionization cross sections for a wide variety of atomic species over a practically relevant range of impact energies. Given the inherent complexity of the problem, a fully quantum mechanical treatment is currently feasible only for the simplest atoms, such as hydrogen and helium.

To gain deeper insights into the ionization mechanisms induced by electron impact, we employ hydrogen atoms as target systems. Ionization by fast particles was first planned quantum mechanically by Bethe [1]. For more than four decades,

extensive research has focused on understanding the ionization process in hydrogen, particularly concerning both ground states [2]-[4] and metastable states [5]-[12]. The double differential cross-section (DDCS) for ground state hydrogen atoms has been comprehensively studied through (e, 2e) experiments, with both theoretical and experimental approaches making significant contributions to the field. Similarly, DDCS studies for hydrogenic metastable 3S-states. In this study, we aim to fill this gap by evaluating the DDCS for electron impact ionization of hydrogen atoms in the meta-stable 3S-state under various kinematic condition, our analysis is based on the multiple scattering theories developed by Das and Seal [2].

The results presented here aim to enhance the understanding of ionization processes in hydrogenic metastable states. Additionally, we compare those of established theories and results [13]-[15]. Lewis integral [16] is used in the present study for analytic calculation. The present new theoretical study on hydrogen 3S-state ionization by electrons offers an immense opportunity for further experimental study for ionization of hydrogen meta-stable 3S-state by electron.

2. Theory

The ionization cross section is the measure of the probability of the ionization process of an atom by electrons or molecule. Electrons impact ionization cross-section is estimated by taking the ratio of the number of ionization elements per unit time and per unit target to the incident electron flux. In this theory, we used the multiple scattering theories of Das and Seal [2]. The ionization of atomic hydrogen by electron in the most elaborate form is presently available in the following type

$$\mathrm{e}^{-}+\mathrm{H}(3\mathrm{S})\rightarrow \mathrm{H}^{+}+2\mathrm{e}^{-} \tag{1}$$

The symbol 3S represents the hydrogen meta-stable state and has been investigated in co-planar geometry through the analysis of Triple Differential Cross Sections (TDCS) obtained from (e, 2e) coincidence experiments. The direct T-matrix element for the ionization of hydrogen atoms by electron impact [2] can be expressed as

$$T_{FI}=\left\langle \Psi_{F}^{(-)}\left(\overline{\gamma}_{a},\overline{\gamma}_{b}\right)\middle|V_{I}\left(\overline{\gamma}_{a},\overline{\gamma}_{b}\right)\middle|\Phi_{I}\left(\overline{\gamma}_{a},\overline{\gamma}_{b}\right)\right\rangle \tag{2}$$

Here the perturbation potential $V_{I}\left(\overline{\gamma}_{a},\overline{\gamma}_{b}\right)$ is given by

$$V_{I}\left(\overline{\gamma}_{a},\overline{\gamma}_{b}\right)=\frac{1}{\gamma_{ab}}-\frac{Z}{\gamma_{b}} \tag{3}$$

The nuclear charge of the hydrogen atom is (Z) = 1, $\overline{\gamma}_{a}$ and $\overline{\gamma}_{b}$ are the distances of the two electrons from the nucleus and γ_{ab} is the distance between the two electrons (see **Figure 1**).

The initial channel unperturbed wave function is

$$\begin{aligned}\Phi_{I}\left(\overline{\gamma}_{a},\overline{\gamma}_{b}\right)&=\frac{\mathrm{e}^{i\cdot\overline{p}_{i}\cdot\overline{\gamma}_{b}}}{(2\pi)^{\frac{3}{2}}}\phi_{3S}\left(\overline{\gamma}_{a}\right)\\&=\frac{\mathrm{e}^{i\cdot\overline{p}_{i}\cdot\overline{\gamma}_{b}}}{(2\pi)^{\frac{3}{2}}}\cdot\frac{1}{81\sqrt{3\pi}}\left(27-18\gamma_{a}+2\gamma_{a}^{2}\right)\mathrm{e}^{-\lambda_{a}\gamma_{a}}\end{aligned} \tag{4}$$

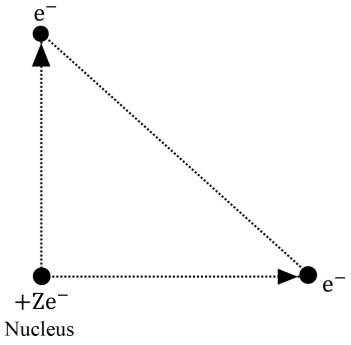

Figure 1. A schematic of the electron-electron and electron-nucleus interactions during ionization.

Here

$$\phi_{3S}\left(\overline{\gamma}_a\right)=\frac{1}{81\sqrt{3\pi}}\left(27-18\gamma_a+2\gamma_a^2\right)\mathrm{e}^{-\lambda_a\gamma_a} \tag{5}$$

Here $\lambda_a=\frac{1}{3}$, $\phi_{3S}\left(\overline{\gamma}_a\right)$ is the hydrogen 3S-state wave function, and $\Psi_F^{(-)}\left(\overline{\gamma}_a,\overline{\gamma}_b\right)$ is the final three-particle scattering state wave function [2] with the electrons being in the continuum with momenta $\overline{p}_a$ and $\overline{p}_b$. And the coordinates of the two electrons are $\overline{\gamma}_a$ and $\overline{\gamma}_b$ respectively. Here the approximate wave function $\Psi_F^{(-)}\left(\overline{\gamma}_a,\overline{\gamma}_b\right)$ is given by

$$\begin{aligned}\Psi_F^{(-)}\left(\overline{\gamma}_a,\overline{\gamma}_b\right)=N\left(\overline{p}_a,\overline{p}_b\right)\Big[&\phi_{\overline{p}_a}^{(-)}\left(\overline{\gamma}_a\right)\mathrm{e}^{i\overline{p}_b\cdot\overline{\gamma}_b}+\phi_{\overline{p}_2}^{(-)}\left(\overline{\gamma}_b\right)\mathrm{e}^{i\overline{p}_a\cdot\overline{\gamma}_a}\\&+\phi_{\overline{p}}^{(-)}\left(\overline{\gamma}\right)\mathrm{e}^{i\overline{P}\cdot\overline{R}}-2\mathrm{e}^{i\overline{p}_a\cdot\overline{\gamma}_a+i\overline{p}_b\cdot\overline{\gamma}_b}\Big]\Big/\left(2\pi\right)^3\end{aligned} \tag{6}$$

Here $\overline{\gamma}=\frac{\overline{\gamma}_b-\overline{\gamma}_a}{2}$, $\overline{R}=\frac{\overline{\gamma}_b+\overline{\gamma}_a}{2}$, $\overline{p}=\left(\overline{p}_b-\overline{p}_a\right)$, $\overline{P}=\left(\overline{p}_b+\overline{p}_a\right)$

Here $N\left(\overline{p}_a,\overline{p}_b\right)$ is the normalization constant, given by,

$$\begin{aligned}&\left|N\left(\overline{p}_a,\overline{p}_b\right)\right|^{-2}\\&=\left|7-2\left[\lambda_a+\lambda_b+\lambda_c\right]-\left[\frac{2}{\lambda_a}+\frac{2}{\lambda_b}+\frac{2}{\lambda_c}\right]+\left[\frac{\lambda_a}{\lambda_b}+\frac{\lambda_a}{\lambda_c}+\frac{\lambda_b}{\lambda_a}+\frac{\lambda_b}{\lambda_c}+\frac{\lambda_c}{\lambda_a}+\frac{\lambda_c}{\lambda_b}\right]\right|\end{aligned} \tag{7}$$

Here

$$\lambda_a=\mathrm{e}^{\frac{\pi\alpha_a}{2}\Gamma\left(1-i\alpha_a\right)},\quad \alpha_a=\frac{1}{p_a}$$

$$\lambda_b=\mathrm{e}^{\frac{\pi\alpha_b}{2}\Gamma\left(1-i\alpha_b\right)},\quad \alpha_b=\frac{1}{p_b}$$

$$\lambda_c=\mathrm{e}^{\frac{\pi\alpha}{2}\Gamma\left(1-i\alpha\right)},\quad \alpha=-\frac{1}{p}$$

And $\phi_{\overline{q}}^{(-)}\left(\overline{\gamma}\right)$ is the coulomb wave function, given by,

$$\phi_{\overline{q}}^{(-)}\left(\overline{\gamma}\right)=\mathrm{e}^{\frac{\pi\alpha}{2}}\Gamma\left(1+i\alpha\right)\mathrm{e}^{i\overline{q}\cdot\overline{\gamma}}\,{}_1F_1\left(-i\alpha,1,-i\left[q\gamma+\overline{q}\cdot\overline{\gamma}\right]\right)$$

The general one-dimensional integral representation of confluent hyper geo-

metric function is written by,

$$ {}_1F_1(a,c,z)=\frac{\Gamma(c)}{(a)\Gamma(c-a)}\int_0^1 \mathrm{d}x x^{(a-1)}(1-x)^{(c-a-1)}\mathrm{e}^{(xz)} $$

For the electron impact ionization, the parameters α_a, α_b and α are given below,

With $\alpha_a=\frac{1}{P_a}$ for $\overline{q}=\overline{p}_a$, $\alpha_b=\frac{1}{p_b}$ for $\overline{q}=\overline{p}_b$ and $\alpha=-\frac{1}{p}$ for $\overline{q}=\overline{p}$.

For the normalization constant $N(\overline{p}_a,\overline{p}_b)$ of Equation (7) has been calculated numerically.

Now applying Equations (3), (4), (5) and (6) to the Equation (2), we get

$$ T_{FI}=N(\overline{p}_a,\overline{p}_b)\left[T_B+T_{B'}+T_I-2T_{PB}\right] \tag{8} $$

where

$$ T_B=\left\langle \Phi^{(-)}_{\overline{p}_a}(\overline{\gamma}_a)\mathrm{e}^{i\overline{p}_b\cdot\overline{\gamma}_b}\middle|V_I\middle|\Phi_I(\overline{\gamma}_a,\overline{\gamma}_b)\right\rangle \tag{9} $$

$$ T_{B'}=\left\langle \Phi^{(-)}_{\overline{p}_b}(\overline{\gamma}_b)\mathrm{e}^{i\overline{p}_a\cdot\overline{\gamma}_a}\middle|V_I\middle|\Phi_I(\overline{\gamma}_a,\overline{\gamma}_b)\right\rangle \tag{10} $$

$$ T_I=\left\langle \Phi^{(-)}_{\overline{p}}(\overline{\gamma})\mathrm{e}^{i\cdot\overline{P}\cdot\overline{R}}\middle|V_I\middle|\Phi_I(\overline{\gamma}_a,\overline{\gamma}_b)\right\rangle \tag{11} $$

$$ T_{PB}=\left\langle \mathrm{e}^{i\overline{p}_a\cdot\overline{\gamma}_a+i\overline{p}_b\cdot\overline{\gamma}_b}\middle|V_I\middle|\Phi_I(\overline{\gamma}_a,\overline{\gamma}_b)\right\rangle \tag{12} $$

For the first-born approximation, Equation (9) may be written as

$$ \begin{aligned} T_B &= \frac{1}{162\sqrt{6}\pi^2}\Phi^{(-)}_{\overline{p}_a}(\overline{\gamma}_a)\mathrm{e}^{i\cdot\overline{p}_b\cdot\overline{\gamma}_b}\left|\frac{1}{\gamma_{ab}}-\frac{1}{\gamma_b}\right|\mathrm{e}^{i\cdot\overline{p}_i\cdot\overline{\gamma}_b}\left(27-18\gamma_a+2\gamma_a^2\right)\mathrm{e}^{-\lambda_a\gamma_a} \\ &= \frac{1}{162\sqrt{6}\pi^2}\int\phi^{(-)*}_{\overline{p}_a}(\overline{\gamma}_a)\mathrm{e}^{-i\cdot\overline{p}_b\cdot\overline{\gamma}_b}\left|\frac{1}{\gamma_{ab}}-\frac{1}{\gamma_b}\right|\mathrm{e}^{i\cdot\overline{p}_i\cdot\overline{\gamma}_b}\left(27-18\gamma_a+2\gamma_a^2\right)\mathrm{e}^{-\lambda_a\gamma_a}\mathrm{d}^3\gamma_a\mathrm{d}^3\gamma_b \\ &= \frac{1}{6\sqrt{6}\pi^2}\int\phi^{(-)*}_{\overline{p}_a}(\overline{\gamma}_a)\mathrm{e}^{-i\cdot\overline{p}_b\cdot\overline{\gamma}_b}\frac{1}{\gamma_{ab}}\mathrm{e}^{i\cdot\overline{p}_i\cdot\overline{\gamma}_b}\mathrm{e}^{-\lambda_a\gamma_a}\mathrm{d}^3\gamma_a\mathrm{d}^3\gamma_b \\ &\quad -\frac{1}{9\sqrt{6}\pi^2}\int\phi^{(-)*}_{\overline{p}_a}(\overline{\gamma}_a)\mathrm{e}^{-i\cdot\overline{p}_b\cdot\overline{\gamma}_b}\frac{\gamma_a}{\gamma_{ab}}\mathrm{e}^{i\cdot\overline{p}_i\cdot\overline{\gamma}_b}\mathrm{e}^{-\lambda_a\gamma_a}\mathrm{d}^3\gamma_a\mathrm{d}^3\gamma_b \\ &\quad +\frac{1}{81\sqrt{6}\pi^2}\int\phi^{(-)*}_{\overline{p}_a}(\overline{\gamma}_a)\mathrm{e}^{-i\cdot\overline{p}_b\cdot\overline{\gamma}_b}\frac{\gamma_a^2}{\gamma_{ab}}\mathrm{e}^{i\cdot\overline{p}_i\cdot\overline{\gamma}_b}\mathrm{e}^{-\lambda_a\gamma_a}\mathrm{d}^3\gamma_a\mathrm{d}^3\gamma_b \\ &\quad -\frac{1}{6\sqrt{6}\pi^2}\int\phi^{(-)*}_{\overline{p}_a}(\overline{\gamma}_a)\mathrm{e}^{-i\cdot\overline{p}_b\cdot\overline{\gamma}_b}\frac{1}{\gamma_b}\mathrm{e}^{i\cdot\overline{p}_i\cdot\overline{\gamma}_b}\mathrm{e}^{-\lambda_a\gamma_a}\mathrm{d}^3\gamma_a\mathrm{d}^3\gamma_b \\ &\quad +\frac{1}{9\sqrt{6}\pi^2}\int\phi^{(-)*}_{\overline{p}_a}(\overline{\gamma}_a)\mathrm{e}^{-i\cdot\overline{p}_b\cdot\overline{\gamma}_b}\frac{\gamma_a}{\gamma_b}\mathrm{e}^{i\cdot\overline{p}_i\cdot\overline{\gamma}_b}\mathrm{e}^{-\lambda_a\gamma_a}\mathrm{d}^3\gamma_a\mathrm{d}^3\gamma_b \\ &\quad -\frac{1}{81\sqrt{6}\pi^2}\int\phi^{(-)*}_{\overline{p}_a}(\overline{\gamma}_a)\mathrm{e}^{-i\cdot\overline{p}_b\cdot\overline{\gamma}_b}\frac{\gamma_a^2}{\gamma_b}\mathrm{e}^{i\cdot\overline{p}_i\cdot\overline{\gamma}_b}\mathrm{e}^{-\lambda_a\gamma_a}\mathrm{d}^3\gamma_a\mathrm{d}^3\gamma_b \\ &\quad T_B=T_{B_1}+T_{B_2}+T_{B_3}+T_{B_4}+T_{B_5}+T_{B_6} \end{aligned} \tag{13} $$

where

$$ T_{B_1}=\frac{1}{6\sqrt{6}\pi^2}\int\phi^{(-)*}_{\overline{p}_a}(\overline{\gamma}_a)\mathrm{e}^{-i\cdot\overline{p}_b\cdot\overline{\gamma}_b}\frac{1}{\gamma_{ab}}\mathrm{e}^{i\cdot\overline{p}_i\cdot\overline{\gamma}_b}\mathrm{e}^{-\lambda_a\gamma_a}\mathrm{d}^3\gamma_a\mathrm{d}^3\gamma_b \tag{14} $$

$$T_{B_2} = -\frac{1}{9\sqrt{6}\pi^2}\int \phi_{\bar{p}_a}^{(-)*}(\bar{\gamma}_a)\mathrm{e}^{-i\cdot\bar{p}_b\cdot\bar{\gamma}_b}\frac{\gamma_a}{\gamma_{ab}}\mathrm{e}^{i\cdot\bar{p}_i\cdot\bar{\gamma}_b}\mathrm{e}^{-\lambda_a\gamma_a}\mathrm{d}^3\gamma_a\mathrm{d}^3\gamma_b \tag{15}$$

$$T_{B_3} = \frac{1}{81\sqrt{6}\pi^2}\int \phi_{\bar{p}_a}^{(-)*}(\bar{\gamma}_a)\mathrm{e}^{-i\cdot\bar{p}_b\cdot\bar{\gamma}_b}\frac{\gamma_a^2}{\gamma_{ab}}\mathrm{e}^{i\cdot\bar{p}_i\cdot\bar{\gamma}_b}\mathrm{e}^{-\lambda_a\gamma_a}\mathrm{d}^3\gamma_a\mathrm{d}^3\gamma_b \tag{16}$$

$$T_{B_4} = -\frac{1}{6\sqrt{6}\pi^2}\int \phi_{\bar{p}_a}^{(-)*}(\bar{\gamma}_a)\mathrm{e}^{-i\cdot\bar{p}_b\cdot\bar{\gamma}_b}\frac{1}{\gamma_b}\mathrm{e}^{i\cdot\bar{p}_i\cdot\bar{\gamma}_b}\mathrm{e}^{-\lambda_a\gamma_a}\mathrm{d}^3\gamma_a\mathrm{d}^3\gamma_b \tag{17}$$

$$T_{B_5} = \frac{1}{9\sqrt{6}\pi^2}\int \phi_{\bar{p}_a}^{(-)*}(\bar{\gamma}_a)\mathrm{e}^{-i\cdot\bar{p}_b\cdot\bar{\gamma}_b}\frac{\gamma_a}{\gamma_b}\mathrm{e}^{i\cdot\bar{p}_i\cdot\bar{\gamma}_b}\mathrm{e}^{-\lambda_a\gamma_a}\mathrm{d}^3\gamma_a\mathrm{d}^3\gamma_b \tag{18}$$

$$T_{B_6} = -\frac{1}{81\sqrt{6}\pi^2}\int \phi_{\bar{p}_a}^{(-)*}(\bar{\gamma}_a)\mathrm{e}^{-i\cdot\bar{p}_b\cdot\bar{\gamma}_b}\frac{\gamma_a^2}{\gamma_b}\mathrm{e}^{i\cdot\bar{p}_i\cdot\bar{\gamma}_b}\mathrm{e}^{-\lambda_a\gamma_a}\mathrm{d}^3\gamma_a\mathrm{d}^3\gamma_b \tag{19}$$

Here $T_{B_4}=0$ and $T_{B_5}=0$, (for orthogonality condition).

Since electron-nucleus interaction $\frac{1}{\gamma_b}$ does not contribute to first born term; because of the orthogonality of the initial and final target states. The above equations may be written by using Bethe integral [1], as

$$T_{B_1} = \frac{4\mathrm{e}^{\left(\frac{\pi\alpha_a}{2}\right)}\Gamma(1-i\alpha_a)\left(\bar{t}^2-\bar{p}_a\cdot\bar{t}-i\alpha_a\bar{p}_a\cdot\bar{t}\right)\mathrm{e}^{(i\alpha_a\ln\omega)}}{3\sqrt{6}t^2\left\{\bar{t}^2-\left(i\lambda_a+\bar{p}_a\right)^2\right\}\left\{\lambda_a^2+\left(\bar{t}-\bar{p}_a\right)^2\right\}^{2-i\alpha_a}} \tag{20}$$

$$\begin{aligned}T_{B_2} &= \frac{16\sqrt{2}\mathrm{e}^{\left(\frac{\pi\alpha_a}{2}\right)}\Gamma(1-i\alpha_a)\left(\bar{t}^2-\bar{p}_a\cdot\bar{t}-i\alpha_a\bar{p}_a\cdot\bar{t}\right)\mathrm{e}^{(i\alpha_a\ln\omega)}}{3^{\frac{5}{2}}t^2\left\{\bar{t}^2-\left(i\lambda_a+\bar{p}_a\right)^2\right\}\left\{\lambda_a^2+\left(\bar{t}-\bar{p}_a\right)^2\right\}^2}\\ &= \left[\frac{1}{\lambda_a}-\frac{4\lambda_a}{{\lambda_a}^2+\left(\bar{p}_a-\bar{t}\right)^2}-\frac{2\alpha_a\bar{p}_a\left(\lambda_a^2-p_a^2+t^2\right)}{\left(\lambda_a^2-p_a^2+t^2\right)^2+4\lambda_a^2p_a^2}+\frac{4\alpha_a\lambda_a^2p_a}{\left(\lambda_a^2-p_a^2+t^2\right)^2+4\lambda_a^2p_a^2}\right]\\ &\quad +i\left[\frac{2\lambda_a\alpha_a}{\lambda_a^2+\left(\bar{p}_a-\bar{t}\right)^2}-\frac{4\alpha_a\lambda_ap_a^2}{\left(\lambda_a^2-p_a^2+t^2\right)^2+4\lambda_a^2p_a^2}-\frac{2\lambda_a\alpha_a\left(\lambda_a^2-p_a^2+t^2\right)}{\left(\lambda_a^2-p_a^2+t^2\right)^2+4\lambda_a^2p_a^2}\right]\end{aligned} \tag{21}$$

$$T_{B_3} = \frac{4\mathrm{e}^{\left(\frac{\pi\alpha_a}{2}\right)}\Gamma(1-i\alpha_a)\left(\bar{t}^2-\bar{p}_a\cdot\bar{t}-i\alpha_a\bar{p}_a\cdot\bar{t}\right)\mathrm{e}^{(i\alpha_a\ln\omega)}}{81\sqrt{2}\pi t^2\left\{\bar{t}^2-\left(i\lambda_a+\bar{p}_a\right)^2\right\}\left\{\lambda_a^2+\left(\bar{t}-\bar{p}_a\right)^2\right\}^{1+\alpha_a}} \tag{22}$$

$$T_{B_4}=0 \tag{23}$$

$$T_{B_5}=0 \tag{24}$$

$$T_{B_6} = -\frac{8\mathrm{e}^{\left(\frac{\pi\alpha_a}{2}\right)}\Gamma(1-i\alpha_a)\left(\bar{t}^2-\bar{p}_a\cdot\bar{t}-i\alpha_a\bar{p}_a\cdot\bar{t}\right)\mathrm{e}^{(i\alpha_a\ln\omega)}}{81\sqrt{2}\pi t^2\left\{\bar{t}^2-\left(i\lambda_a+\bar{p}_a\right)^2\right\}\left\{\lambda_a^2+\left(\bar{t}-\bar{p}_a\right)^2\right\}^{2-i\alpha_a}} \tag{25}$$

Here $\omega=\frac{\lambda_a^2+\left(\bar{t}-\bar{p}_a\right)^2}{\bar{t}^2-\left(i\lambda_a+\bar{p}_a\right)^2}$ with $\bar{t}=\bar{p}_i-\bar{p}_b$.

$$\begin{aligned}\overline{p}_a \cdot \overline{t} &= \overline{p}_a \cdot \left(\overline{p}_i - \overline{p}_b\right) \\ &= \overline{p}_a \cdot \overline{p}_i - \overline{p}_a \cdot \overline{p}_b \\ &= p_a p_i \cos\theta_a - p_a p_b \cos\theta_{ab}\end{aligned}$$

Here $\cos\theta_{ab} = \cos\theta_a \cos\theta_b - \sin\theta_a \sin\theta_b$

For phase ξ value we have

$$\Gamma\left(1+i\alpha_a\right) = \mathrm{e}^{i\xi}\left|\Gamma\left(1+i\alpha_a\right)\right|$$

$$\Gamma\left(1-i\alpha_a\right) = \mathrm{e}^{-i\xi}\left|\Gamma\left(1-i\alpha_a\right)\right|$$

$$\left|\Gamma\left(1-i\alpha_a\right)\right| = \sqrt{\Gamma\left(1-i\alpha_a\right)\Gamma\left(1+i\alpha_a\right)}$$

$$= \sqrt{\frac{i\alpha_a\pi}{\sin\left(i\alpha_a\pi\right)}}$$

$$= \sqrt{\frac{i\alpha_a\pi}{i\sinh\left(i\alpha_a\pi\right)}}$$

$$\left|\Gamma\left(1-i\alpha_a\right)\right| = \sqrt{\frac{2\pi\alpha_a}{\mathrm{e}^{\pi\alpha_a} - \mathrm{e}^{-\pi\alpha_a}}}$$

Taking the value of (20), (21), (22), (23), (24) and (25) in Equation (13) we find the final value of T_B for First-Born result calculating in this work of Dhar *et al.* [8]. Following analytical evaluations using the Lewis integral [16], the above expressions of Equation (13) has been calculated numerically.

Now, the Triple Differential Cross Section (TDCS) corresponding to the T-matrix element is given by:

$$\frac{\mathrm{d}^3\sigma}{\mathrm{d}E_a \mathrm{d}\Omega_a \mathrm{d}\Omega_b} = \frac{p_a p_b}{p_i}\left|T_{FI}\right|^2 \tag{26}$$

For First-Born approximation we consider $T_{FI} = T_B$

Here the triple differential cross section (TDCS) is denoted by the symbol $\frac{\mathrm{d}^3\sigma}{\mathrm{d}E_a \mathrm{d}\Omega_a \mathrm{d}\Omega_b}$ and E_a is the energy of the ejected electron. Now the double differential cross section (DDCS) is obtained by integrating [8] Equation (26) with respect to solid angle Ω_b.

$$\frac{\mathrm{d}^2\sigma}{\mathrm{d}E_a \mathrm{d}\Omega_a} = \int \frac{\mathrm{d}^3\sigma}{\mathrm{d}E_a \mathrm{d}\Omega_a \mathrm{d}\Omega_b}\mathrm{d}\Omega_b \tag{27}$$

Hence, the resulting expressions were numerically computed using a programming language MATLAB.

3. Results and Discussion

The ionization of hydrogen meta-stable 3S-state by electron impact is presented for different kinematic conditions. The existent new results are assimilated with the hydrogen ground state theoretical results [13] and the absolute data [15]. The Ionization results of hydrogen meta-stable 3d-state [12] and 2S-state result [14] are also covered here for comparison with our new theoretical study results. The

emitted angle θ_a varies from 0˚ to 180˚ considered as a horizontal axis where DDCS is the vertical axis in all figures and the scattered angle θ_b varies from 0˚ to 100˚. The incident electron energy $E_I = 250$ eV and 150 eV at taken here. In all diagram, θ_a (0˚ - 90˚) and $\phi = 0^\circ$ is indicated as recoil fields while θ_a (90˚ - 180˚) and $\phi = 180^\circ$ is referred as binary fields.

The DDCS for the ionization of meta-stable 3S-state hydrogen atoms by electrons at high incident energy of $E_I = 250$ eV and 150 eV are presented (see Figures 2-7).

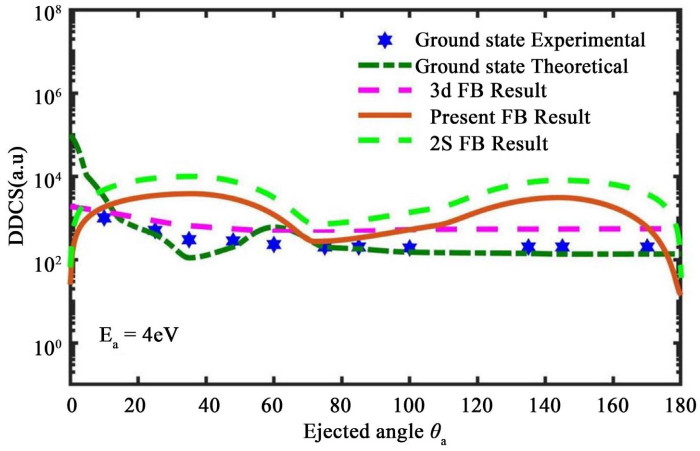

Figure 2. Double Differential Cross Sections (DDCS) versus ejected electron angle θ_a for electron impact energy $E_I = 250$ eV, ejected electron energy $E_a = 4$ eV. Theory: Blue star symbols: Ground state experiment [15], Solid orange curve: Present 3S First Born result, dashed green curve: 2S first-born Result [14], dashed Dark green curve: Ground State theoretical [13], dashed pink curve: 3d-state first-born result [12].

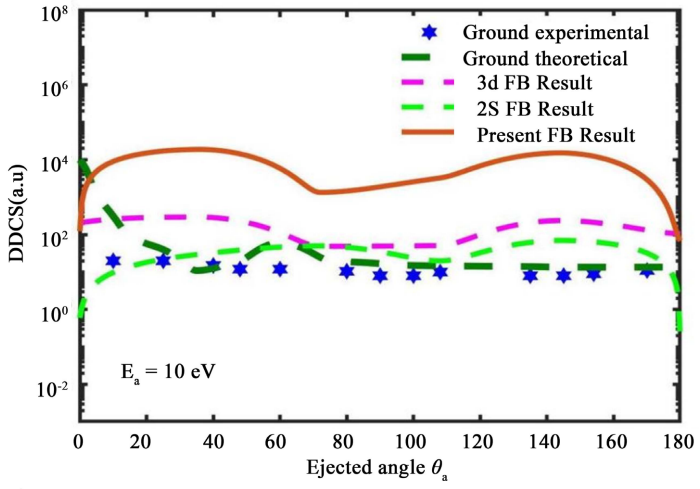

Figure 3. Double Differential Cross Sections (DDCS) versus ejected electron angle θ_a for electron impact energy $E_I = 250$ eV, ejected electron energy $E_a = 10$ eV. Theory: Blue star symbols: Ground state experiment [15], Solid orange curve: Present 3S First-Born result, dashed green curve: 2S first-born Result [14], dashed Dark green curve: Ground State theoretical [13], dashed pink curve: 3d-state first-born result [12].

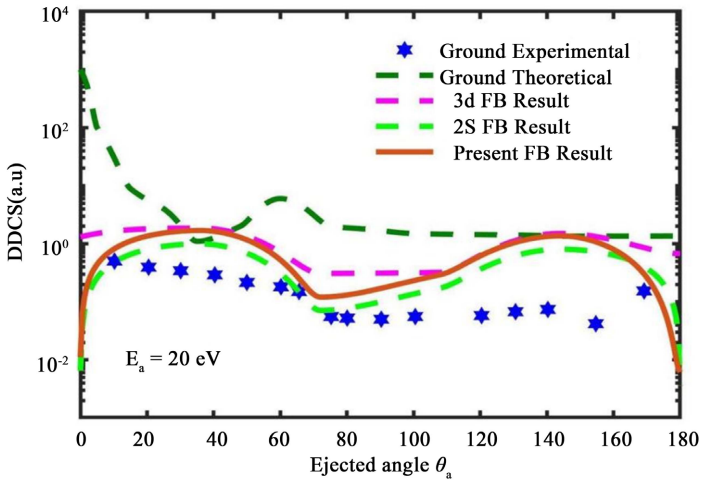

Figure 4. Double Differential Cross Sections (DDCS) versus ejected electron angle θ_a for electron impact energy $E_I = 250$ eV, ejected electron energy $E_a = 20$ eV. Theory: Blue star symbol: Ground state experiment [15], Solid orange curve: Present 3S First-Born result, dashed green curve: 2S first-born Result [14], dashed Dark green curve: Ground State theoretical [13], dashed pink curve: 3d-state first-born result [12].

For an incident energy $E_I = 250$ eV in **Figure 2**, the present results exhibit two distinct peaks in the recoil and binary regions, consistent with the 2S-state results reported in [14]. The current first-born approximation results coincide with those for the ground state in [13] at angles $\theta_a = 10^\circ$, $\theta_a = 70^\circ$ and $\theta_a = 177^\circ$. Moreover, the current result aligns well with the experimental ground state results from [15] in the ejected electron angular range of $\theta_a = 70^\circ$ to $\theta_a = 100^\circ$.

In **Figure 3**, at an ejection energy $E_a = 10$ eV, the present outcome intersects with the ground state result [13] at $\theta_a = 10^\circ$ and with the 3d-state results [12] at both $\theta_a = 10^\circ$ and $\theta_a = 180^\circ$. Furthermore, it crosses the ground state experimental values [15] three times, approximately at $\theta_a = 80^\circ$, $\theta_a = 90^\circ$, $\theta_a = 170^\circ$, indicating a good overall assessment. Additionally, while the present results and the 2S-state result [14] exhibit a similar shape throughout the entire angular region, they differ in magnitude.

In **Figure 4**, $E_a = 20$ eV, the current result shows, the current result show similar nature specially in the recoil region with ground state experimental result [15], 3d-state result [12] and 2S-state result [14] but in the binary region it is not agree well with experimental result [15] due to different state. It meets with ground state theoretical result [13] at ejected angles 30˚, 50˚, and 150˚.

For incident energy $E_I = 150$ eV, as shown in **Figure 5**, the present results, along with the 3d-state result [12] and the 2S-state result [14], exhibit similar shapes in both the recoil and binary regions, though with differing magnitudes. The current first-born approximation results coincide with the ground state theoretical result [13] at angles $\theta_a = 10^\circ$ and $\theta_a = 180^\circ$. Furthermore, the present results align well with the experimental ground state data from [15] in the ejected

electron angular range of $\theta_a = 70^\circ$ to $\theta_a = 100^\circ$.

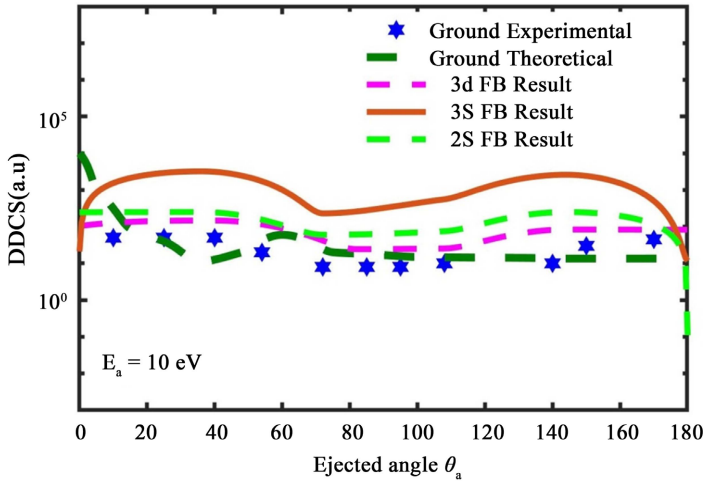

Figure 5. Double-differential cross sections (DDCS) versus ejected electron angle θ_a for electron impact energy $E_I = 250$ eV, ejected electron energy 10 eV. Theory: Blue star symbols: Ground state experiment [15], Solid orange curve: Present 3S First-Born result, dashed green curve: 2S first-born Result [14], dashed Dark green curve: Ground State theoretical [13], dashed pink curve: 3d-state first-born result [12].

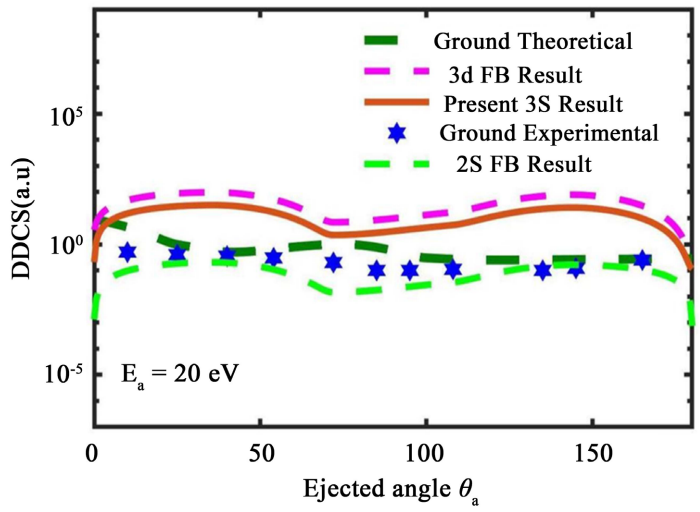

Figure 6. Double Differential Cross Sections (DDCS) versus ejected electron angle θ_a for electron impact energy $E_I = 250$ eV, ejected electron energy $E_a = 20$ eV. Theory: Blue star symbols: Ground state experiment [15], Solid orange curve: Present 3S First-Born result, dashed green curve: 2S first-born Result [14], dashed Dark green curve: Ground State theoretical [13], dashed pink curve: 3d-state first born result [12].

Let us consider the case of **Figure 6**, the current Double Differential Cross Section (DDCS) result and the 3d-state results [12] exhibit a similar shape in the recoil and binary regions but differ in magnitude from the 2S-state results [14]. Notably, the present DDCS results share a similar pattern, especially in the recoil region, with both the ground state results [13] and the corresponding experi-

mental results [15]. However, in the binary region, there is a lack of agreement with those results [13] [15] due to the different states involved.

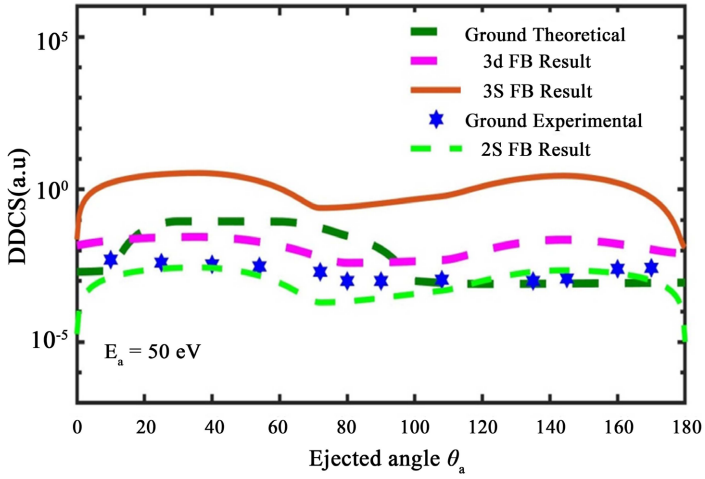

Figure 7. Double Differential Cross Sections (DDCS) versus ejected electron angle θ_a for electron impact energy $E_I = 250$ eV, ejected electron energy $E_a = 50$ eV. Theory: Blue star symbols: Ground state experiment [15], Solid orange curve: Present 3S First-Born result, dashed green curve: 2S first-born Result [14], dashed Dark green curve: Ground State theoretical [13], dashed pink curve: 3d-state first-born result [12].

At last, we consider ejection energy as $E_a = 50$ eV, in **Figure 7**, The present calculation and the 3d-state meta-stable result from [12] show a similar shape to the ground state theoretical result [13] in the recoil region, while differing notably in the binary region. The present DDCS magnitudes are higher than those of the ground state experiment [15] and 2S-state result [14] in both regions.

Here is a table (see **Table 1**) of comparison results for ionization of hydrogen 3S-state for incident energy $E_I = 250$ eV is presented.

Table 1. DDCS results for ejected angles θ_a corresponding to various scattering angles θ_b for $E_a = 4$ eV, $E_a = 10$ eV, $E_a = 20$ eV in ionization of hydrogen atoms for 250 eV.

θ_a (deg)	θ_b (deg)	DDCS $E_a = 4$ eV	DDCS $E_a = 10$ eV	DDCS $E_a = 20$ eV
0	0	0.0250E−03	0.0124E−04	0.0111
1	36	3.8110E−03	1.8864E−04	1.6932
2	72	0.2716E−03	0.1345E−04	0.1207
4	108	0.6601E−03	0.3267E−04	0.2933
10	144	3.0789E−03	1.5240E−04	1.3679
20	180	0.0139E−03	0.0069E−04	0.0062
30	216	4.3356E−03	2.1461E−04	1.9263
40	252	0.0690E−03	0.0342E−04	0.0307

Continued

60	288	1.2456E−03	0.6166E−04	0.5534
90	324	2.2606E−03	1.1190E−04	1.0044
100	360	0	0	0

Finally, meta stable 3S-state is an excited state of an atom or other system with a longer lifetime than the other excited states. However, it has a shorter lifetime than the stable ground state. The peak structure of the present results shows good qualitative agreement with compared results in the recoil region but shows somewhat disagreement in the binary region. This may have happened due to the change of the hydrogen meta-stable states by electrons. It is remarked that the peak structure for both in recoil and binary region, the First-Born results are very close to the meta-stable 2S-state with different magnitudes for all scattering angles. But in the binary region, the opposite peak patterns of the meta-stable 2S-state [10] are much sharper than the corresponding ground state experimental result [15] and 3S-state results. However, the limitation of the theory is that at low energy, the theory of Das and Seal [2] does not give significant results.

4. Conclusion

This study presents the calculation of Double Differential Cross Sections (DDCS) for the ionization of meta-stable 3S-state hydrogen atoms impacted by electron at incident energies of 150 eV and 250 eV. These new theoretical results significantly contribute to the ongoing exploration of meta-stable state ionization. Currently, no experimental data is available to validate these DDCS results for hydrogen 3S-state. The findings are expected to stimulate further theoretical and experimental efforts to study ionization cross-sections of various meta-stable states in hydrogen due to electron and positron impact. Such studies are vital for advancing our understanding of atomic scattering phenomena. Investigations under different kinematic conditions and for other atomic species would also be of considerable interest.

Acknowledgements

The computational work was conducted in the Simulation Lab, Department of Mathematics, Chittagong University of Engineering and Technology, Chittagong, 4349, Bangladesh.

Conflicts of Interest

The authors state that they have no conflicts of interest related to the publication of this paper.

References

[1] Bethe, H. (1930) On the Theory of the Passage of Fast Corpuscular Rays through Matter. *Annalen der Physik*, **397**, 325-400. https://doi.org/10.1002/andp.19303970303

[2] Das, J.N. and Seal, S. (1993) Electron-Hydrogen-Atom Ionization Collisions at Intermediate ($5I_0$-$20I_0$) and High ($\gtrsim 20I_0$) Energies. *Physical Review A*, **47**, 2978-2986. https://doi.org/10.1103/physreva.47.2978

[3] Berakdar, J. and Klar, H. (1993) Structures in Triply and Doubly Differential Ionization Cross Sections of Atomic Hydrogen. *Journal of Physics B: Atomic, Molecular and Optical Physics*, **26**, 3891-3913. https://doi.org/10.1088/0953-4075/26/21/023

[4] Brauner, M., Briggs, J.S. and Klar, H. (1989) Triply-Differential Cross Sections for Ionisation of Hydrogen Atoms by Electrons and Positrons. *Journal of Physics B: Atomic, Molecular and Optical Physics*, **22**, 2265-2287. https://doi.org/10.1088/0953-4075/22/14/010

[5] Dhar, S. and Nahar, N. (2015) Electron Impact Ionization of Metastable 2P-State Hydrogen Atoms in the Coplanar Geometry. *Results in Physics*, **5**, 3-8. https://doi.org/10.1016/j.rinp.2014.11.001

[6] Dhar, S. and Nahar, N. (2014) Ionization of Metastable 2P-State Hydrogen Atoms by Electron Impact for Coplanar Asymmetric Geometry. *Open Journal of Microphysics*, **4**, 46-53. https://doi.org/10.4236/ojm.2014.44007

[7] Dhar, S. (2015) Energy Spectrum of Ejected Electrons of H(2P) Ionization by Electrons in Coplanar Asymmetric Geometry. *American Journal of Modern Physics*, **4**, 132-137. https://doi.org/10.11648/j.ajmp.20150403.15

[8] Dhar, S. (2015) Electron Impact Ionization of Metastable 3S-State Hydrogen Atoms by Electrons in Coplanar Geometry. *American Journal of Modern Physics*, **4**, 261-266. https://doi.org/10.11648/j.ajmp.20150406.11

[9] Dhar, S., Akter, S. and Nahar, N. (2016) The First Born Triple Differential Cross-Section for Ionization of H(3P) by Electron Impact in the Asymmetric Coplanar Geometry. *Open Journal of Microphysics*, **6**, 15-23. https://doi.org/10.4236/ojm.2016.61002

[10] Shyn, T.W., Sharp, W.E. and Kim, Y.-K. (1981) Doubly Differential Cross Sections of Secondary Electrons Ejected from Gases by Electron Impact: 25-250 eV on H_2. *Physical Review A*, **24**, 79-88. https://doi.org/10.1103/physreva.24.79

[11] Banerjee, S., Dhar, S. and Hoque, A. (2018) Triple Differential Cross-Sections for Ionization of H(3D) by Incident Electron. *Open Journal of Microphysics*, **8**, 30-41. https://doi.org/10.4236/ojm.2018.84005

[12] Banerjee, S. and Dhar, S. (2024) First Born Double Differential Cross-Section for Ionization of H (3D) by Incident Electron Impact. *Open Journal of Microphysics*, **14**, 67-77. https://doi.org/10.4236/ojm.2024.142005

[13] Das, J.N. and Seal, S. (1994) Multiple Scattering Calculation of Double and Single Differential Cross Sections for Ionization of Hydrogen Atoms by Electrons at Intermediate Energies. *Zeitschrift für Physik D Atoms, Molecules and Clusters*, **31**, 167-170. https://doi.org/10.1007/bf01437831

[14] Chowdhury, M.T.H. and Dhar, S. (2023) Double Differential Cross-Section for the Ionization of Hydrogenic 2S Metastable State. *Open Journal of Microphysics*, **13**, 1-13. https://doi.org/10.4236/ojm.2023.131001

[15] Shyn, T.W. (1992) Doubly Differential Cross Sections of Secondary Electrons Ejected from Atomic Hydrogen by Electron Impact. *Physical Review A*, **45**, 2951-2956. https://doi.org/10.1103/physreva.45.2951

[16] Lewis, R.R. (1956) Potential Scattering of High-Energy Electrons in Second Born Approximation. *Physical Review*, **102**, 537-543. https://doi.org/10.1103/physrev.102.537